Earthq Eng & Eng Vib (2009) 8:287-299 **DOI**: 10.1007/s11803-009-9052-1

Three dimensional temporal characteristics of ground motions and building responses in Wenchuan earthquake

Dai Junwu[1†], Wang Yanru[1‡], Guan Qingsong[1§], Qi Xiaozhai[1†], Yang Xueshan[1†], Tong Mai[2†] and George C. Lee[3†]

1. *Institute of Engineering Mechanics, China Earthquake Administration, Harbin 150080, China*
2. *FEMA, Washington DC, USA*
3. *MCEER, University at Buffalo, USA*

Abstract: In this paper, analytical results from 3D temporal characteristics of the responses of an RC frame building subjected to both a large aftershock and the main shock of Wenchuan M_s8.0 earthquake are presented. The ground motion records from the main shock were obtained from three nearby stations. The acceleration records were analyzed in terms of instantaneous tangential acceleration a_T, normal acceleration a_N, Euclidean norm of acceleration vector $|\boldsymbol{a}|$, velocity vector $|\boldsymbol{v}|$, displacement vector $|\boldsymbol{v}|$, temporal curvature κ, κ_t, and temporal torsion γ and γ_t. Results of the kinematic relationship between the above factors and some additional in depth information obtained from extensive analyses are provided and discussed.

Keywords: 3D temporal characteristics analyses; Wenchuan earthquake; RC frame structure; aftershock

1 Introduction

The "5.12" Wenchuan earthquake caused severe damage or collapse to a large number of structures, resulting in thousands of casualties. Most of the casualties and losses were caused by structural damage. Therefore, study of strong ground motions and the performance of structures subjected to earthquake ground shaking are very important. Most currently used ground motions, such as PGA, PGV, and PGD indices, portray the essential kinematic relationship of the 3D time histories, but do not contain sufficient information to differentiate the various causes and formations of damage characteristics of the underlying ground motions (Dai *et al*., 2004; Dai *et al*., 2008). The temporal characteristics, normal and tangential acceleration, and temporal bending and torsion, are useful tools to achieve a better understanding of the unique characteristics of earthquake ground motions and structural responses. Furthermore, they can be especially useful in identifying certain nonlinear dynamics involved in the ground motions and structural responses (Lee *et al*., 2000).

In this paper, a 3D temporal characteristics analysis (Tong and Lee, 1999; Tong *et al*., 2002) is conducted to demonstrate the characteristics of ground motions and seismic responses of an RC frame structure to the largest M_s6.4 aftershock, which occurred on May 25, 2008. During the aftershock, acceleration records of structural responses from an RC frame building were obtained. This was the first time that the jerks (the derivative of acceleration, da/dt) of both the ground shaking and structural responses were recorded during an earthquake event, and the analyses provide necessary and useful information for further study.

Correspondence to: Dai Junwu, Institute of Engineering Mechanics, China Earthquake Administration, 9 Xuefu Road, Harbin 150080, China
Tel: +86-451-86652883
E-mail: jwdai@iem.net.cn
†Professor; ‡PhD Candidate; §Graduate Student

Supported by: NSFC program (No. 50678161); the National Major Basic Research 973 Program Under Grant No. 2007CB714205; the Science and Technology Support Program Under Grant No. 2006BAC13B02-0301 of the Ministry of Science and Technology of China; the Basic Science Research Foundation Program through Institute of Engineering Mechanics, CEA
Received March 30, 2009; **Accepted** April 21, 2009

2 Case study of 3D temporal characteristics of strong motions of M_s8.0 Wenchuan earthquake

2.1 Ground acceleration records nearby Jiangyou

Three sets of ground motion records (obtained from the China National Strong Motion Network Center) during the Wenchuan earthquake from near downtown Jiangyou (see Fig. 1) were selected as examples to evaluate 3D temporal characteristics. Basic information, including location and peak ground accelerations (PGAs), about these records is provided in Tables 1 and 2.

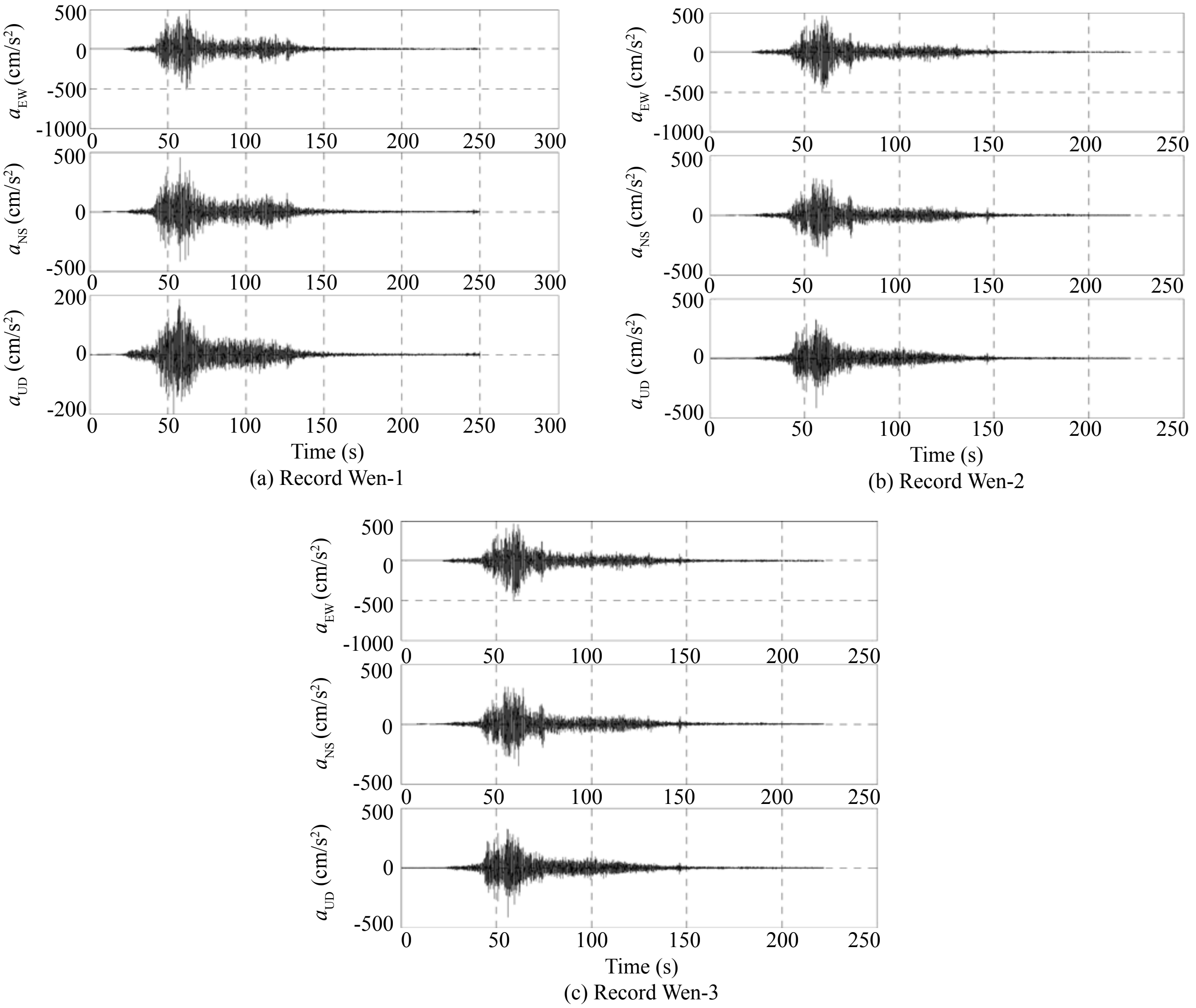

Fig. 1 Ground acceleration time histories recorded from nearby stations

Table 1 Characteristics of selected ground motion records from the great Wenchuan earthquake

Record No.	Stations	Serial number	Latitude (º)	Long. (º)	EW components		NS components		UD components	
					t_{EW} (s)	PGA (cm/s^2)	t_{NS} (s)	PGA (cm/s^2)	t_{UD} (s)	PGA (cm/s^2)
Wen-1	Jiangyou	51JYD	104.7	31.8	62.12	-507.9389	58.12	456.836	53.85	-198.1359
Wen-2	Hanzeng	51JYH	104.6	31.8	59.06	-509.3733	61.855	-350.3079	56.175	-442.9893
Wen-3	Zhonghua	51JYC	105	31.9	57.225	295.7031	55.235	279.7677	68.925	-180.3038

Table 2 Predominant periods of ground motions

Translational components	Predominant periods of the ground motions of records (s)		
	Wen-1	Wen-2	Wen-3
a_{EW}	0.1774	0.1433	0.1864
a_{NS}	0.1516	0.1112	0.1774
a_{UD}	0.08841	0.0526	0.135

2.2 Three dimensional temporal characteristics analyses of the example ground motions

2.2.1 Acceleration and velocity characteristics

Comparisons of the instantaneous tangential acceleration a_T, normal acceleration a_N, the Euclidean norm of acceleration vector $|\boldsymbol{a}|$, velocity vector $|\boldsymbol{v}|$, and displacement vector $|\boldsymbol{d}|$ for three records are summarized in Table 3. Note that peak $|\boldsymbol{d}|$ occurred later than peak $|\boldsymbol{a}|$ and was followed by peak $|\boldsymbol{v}|$; the peaks of $|\boldsymbol{a}|$ and absolute value a_T often arrived almost simultaneously. Furthermore, Fig. 2 shows that a_N arrived at its peak value when a_T was equal to zero. From these observations, it is reasonable to believe that peaks $|\boldsymbol{d}|$, $|\boldsymbol{a}|$, and $|\boldsymbol{v}|$ are kinetically related to each other, and a_T has an essential influence on $|\boldsymbol{a}|$. From Table 3 and Fig. 2, note that large a_T, a_N, and $|\boldsymbol{a}|$ are not always accompanied by large $|\boldsymbol{v}|$, and peak values of the a_T, a_N, and $|\boldsymbol{a}|$ of records Wen-1 and Wen-2 are both larger than Wen-3; however, the peak values of the $|\boldsymbol{v}|$ of both Wen-1 and Wen-2 are less than Wen-3. In addition, the $|\boldsymbol{v}|$ always increases with positive a_T and decreases with negative a_T. These observations suggest that high ground motion acceleration does not always correspond to large velocity or displacement. Instead, a large or long-lasting positive a_T component may be more vulnerable than the peak values of the EW, NS, and UD acceleration components.

2.2.2 Temporal curvature characteristics

The temporal curvature κ is the rate of turning (radian) in per-unit length of S, where S represents the 3D displacement experienced by the point considered on the ground; its reciprocal is the radius of curvature (Tong and Lee, 1999). According to $a_N=\kappa(\mathrm{d}S/\mathrm{d}t)^2=\kappa|\boldsymbol{v}|^2$ (Tong *et al.*, 2006), κ is directly related to a_N as seen from Fig. 3, the maximum κ always corresponds to the maximum a_N and their values approach each other. Furthermore, the maxima of κ and a_N always correspond to the minima of $|\boldsymbol{v}|$, and is also the same for the opposite case. This implies that every curvature pulse results in an increase of normal acceleration and a loss of some velocity. It is amazing that, according to $a_N=\kappa|\boldsymbol{v}|^2$, a_N is proportional to $|\boldsymbol{v}|^2$, but its peak values are often related to the minima of $|\boldsymbol{v}|$ and maximum of κ. This is similar to findings reported in prior research (Tong and Lee, 1999).

Temporal curvature in a unit of time κ_t is obtained by multiplying $|\boldsymbol{v}|$ by κ. From Figs. 3(a)–3(c), note that pulses κ_t and κ vary with time, and are in phase for all three records; however, their amplitudes differ significantly from each other. This indicates that the influence of the velocity is significant.

2.2.3 Temporal torsion characteristics

Temporal torsion γ is the rate of twisting (radian) in per-unit length of S. Its reciprocal is the radius of torsion. According to 3D temporal characteristics theory, γ is closely related to $\mathrm{d}a/\mathrm{d}t$. It involves the information of directional changes in acceleration. Temporal torsion in units of time γ_t is obtained by multiplying $|\boldsymbol{v}|$ and γ. (Tong and Lee, 1999)

Figure 4 presents comparisons of κ, γ, γ_t, and $|\boldsymbol{v}|$. The pulses of γ and γ_t always occur simultaneously; further, they often occur at a time of high velocity, just the opposite of κ pulses. γ and κ are mutually reversed; that is to say, curvature pulses correspond to the torsion valleys and its valleys correspond to the torsion pulse. This observation has been made in prior research (Tong and Lee, 1999).

Table 3 Comparison of a_T, a_N, $|a|$, $|v|$ and $|d|$

Record No.	Responses	Time(s)	Peak values
Wen-1	Positive a_T	62	412.3784 cm/s^2
	Negative a_T	63.96	-570.5367 cm/s^2
	a_N	49.49	461.6245 cm/s^2
	$\|\boldsymbol{a}\|$	63.96	609.4607 cm/s^2
	$\|\boldsymbol{v}\|$	49.78	39.8221 cm/s
	$\|\boldsymbol{d}\|$	50.96	44.8382 cm
Wen-2	Positive a_T	56.93	341.7038 cm/s^2
	Negative a_T	59.33	-390.2559 cm/s^2
	a_N	59.05	519.9636 cm/s^2
	$\|\boldsymbol{a}\|$	59.34	539.6633 cm/s^2
	$\|\boldsymbol{v}\|$	49.54	35.6588 cm/s
	$\|\boldsymbol{d}\|$	50.64	55.0325 cm
Wen-3	Positive a_T	57.22	255.2972 cm/s^2
	Negative a_T	57.33	-237.2189 cm/s^2
	a_N	47.86	314.8068 cm/s^2
	$\|\boldsymbol{a}\|$	57.21	320.7535 cm/s^2
	$\|\boldsymbol{v}\|$	52.98	41.6364 cm/s
	$\|\boldsymbol{d}\|$	56.15	38.6838 cm

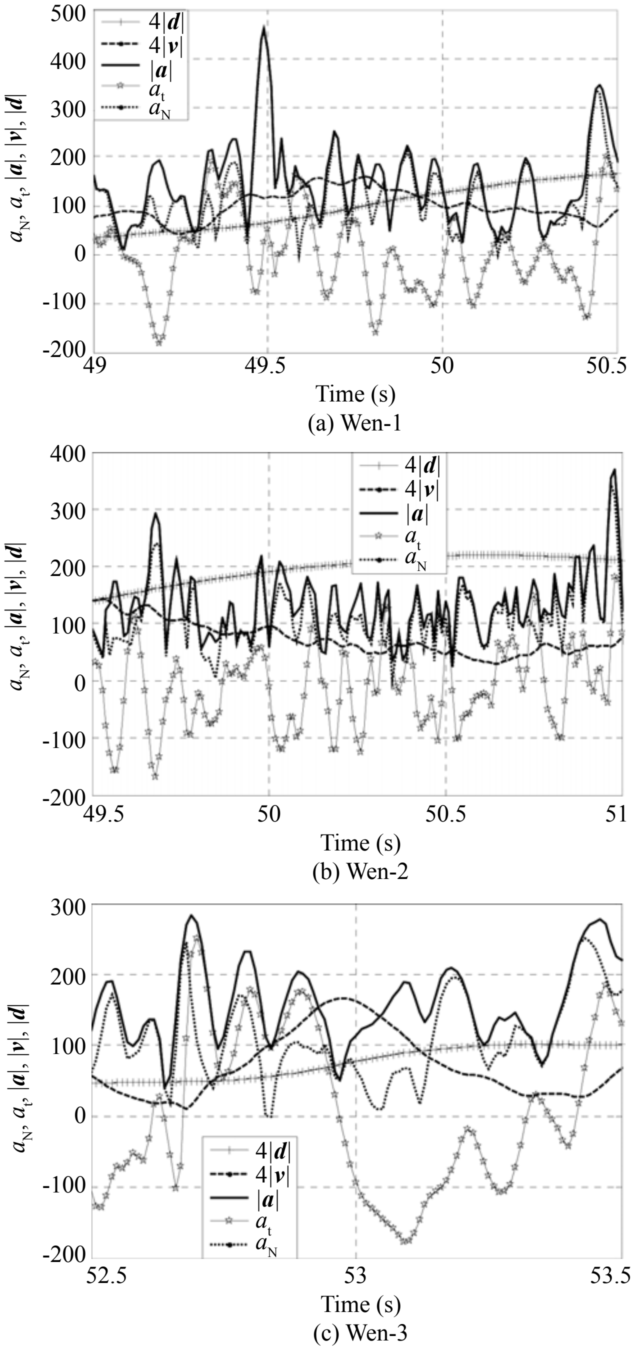

Fig. 2 a_T, a_N, $|a|$, $|v|$ and $|d|$ (a_T (cm/s^2), a_N (cm/s^2), $|a|$ (cm/s^2), $|v|$ (cm/s) and $|d|$ (cm))

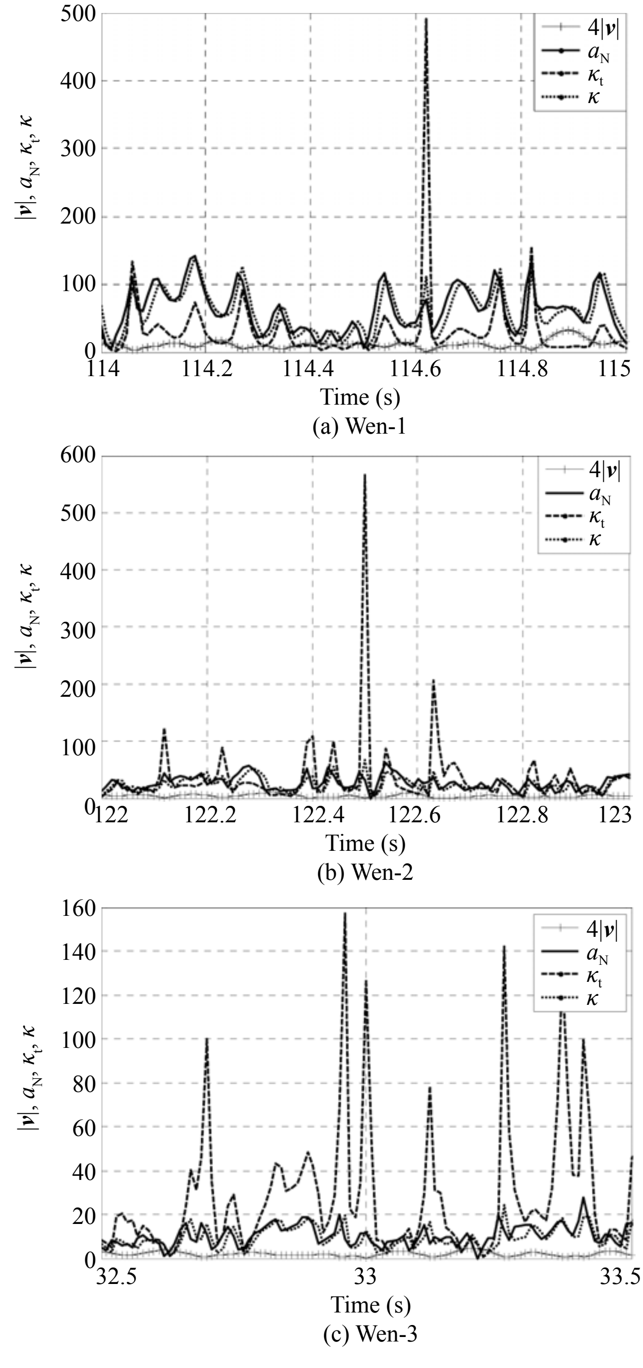

Fig. 3 Comparison of κ, κ_t, a_N, and $|v|$ recorded from nearby stations (κ (rad/cm), κ_t (rad/s), a_N (cm/s^2) and $|v|$(cm/s))

3 Three dimensional temporal characteristics analyses of response of a RC framed building structure

3.1 Description of the RC framed building

The responses of a four-story RC frame office building (Fig. 5) were obtained during a large M_s6.4 aftershock. The dimensions of the building were about 10.8 m × 38 m × 14.4 m (width×length×height). The building belongs to Sichuan Mining Mechanical Corp., located in Jiangyou County, downtown of Sichuan Province in the east, about 40 kilometers away from the major rupture of the Wenchuan earthquake. The local seismic design fortification intensity was VII (PGA, a_{PG}= 0.1g), while the observed intensity was about VIII, and the site class belonged to type I according to the Chinese code for seismic design of buildings.

During the main shock of the Wenchuan earthquake, the RC frame structure of the office building remained intact with slight damage to a few masonry infill walls as shown in Fig. 6. The damage to infill walls was mainly observed on the 1st floor, with light damage on the 2nd, 3rd, and 4th floors. Even though the infill walls

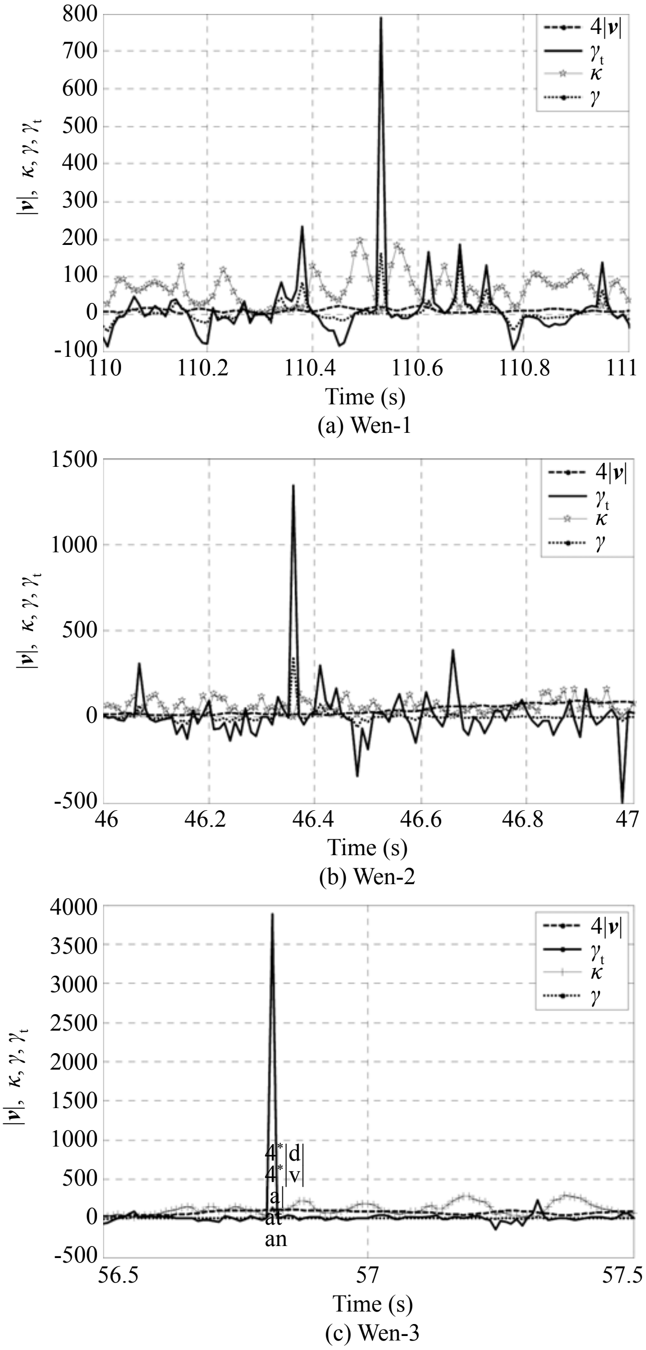

(a) Wen-1

(b) Wen-2

(c) Wen-3

Fig. 4 Comparison of κ, γ, γ_t and $|v|$ recorded from different stations (κ (rad/cm), γ (rad/cm), γ_t (rad/s) and $|v|$ (cm/s))

Fig. 5 Overview of RC frame office building

between the windows on the 2nd, 3rd, and 4th floors were narrower than on the ground floor, they showed less damage. Horizontal cracks on the 4th floor appeared below the beam of the staircase, and wider horizontal cracks occurred on the side of the larger structural bay.

Crack distribution on the 1st floor of the building is shown in Fig. 7.

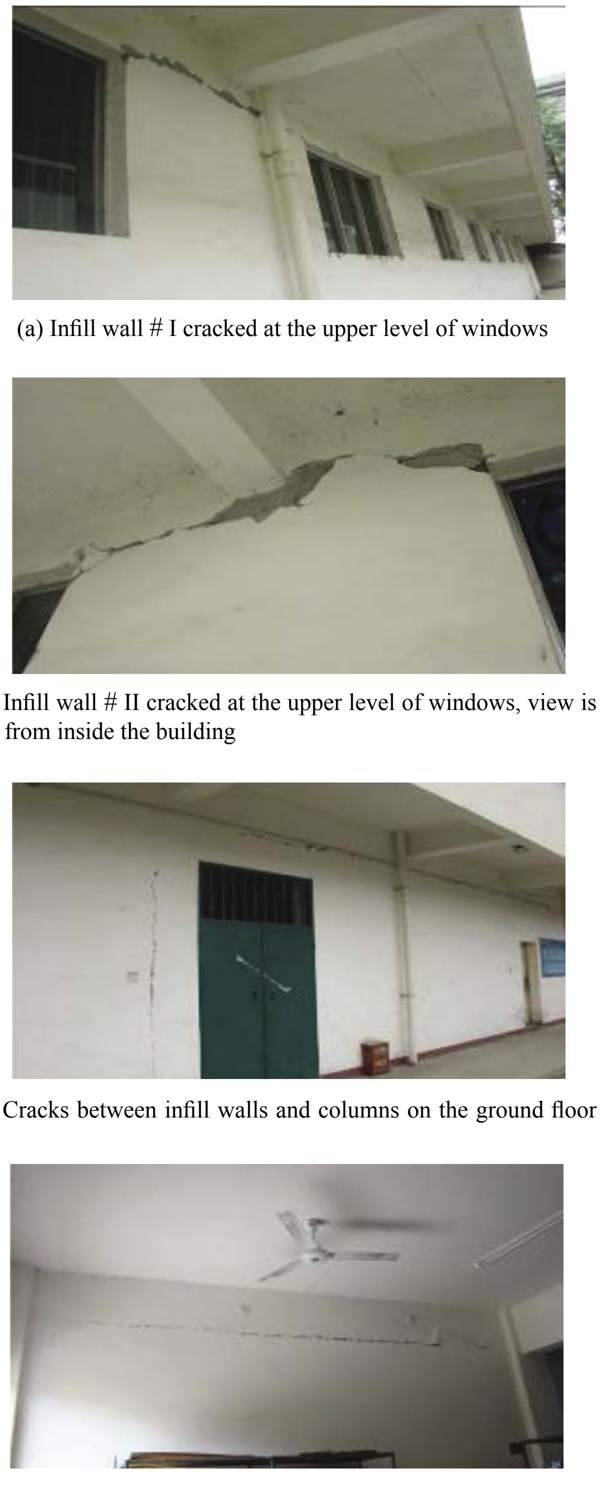

(a) Infill wall # I cracked at the upper level of windows

(b) Infill wall # II cracked at the upper level of windows, view is from inside the building

(c) Cracks between infill walls and columns on the ground floor

(d) Cracks in infill wall below the beam on the ground floor

Fig. 6 Horizontal cracks observed in the RC frame structure

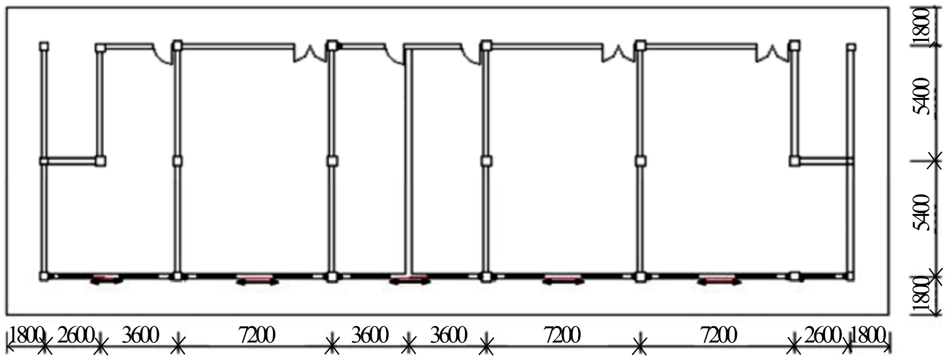

Fig.7 Crack positions projected onto a plan of ground floor. Black spots represent vertical cracks along the intersection of infill wall and column, and arrowhead represents horizontal cracks at the upper level of windows (length unit: mm)

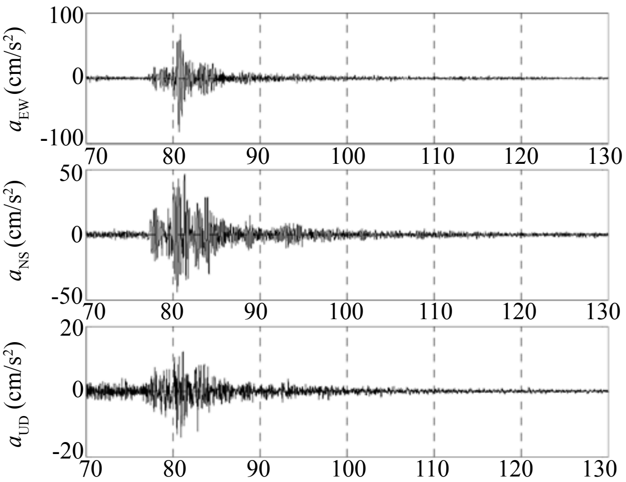

(a) At 4th floor

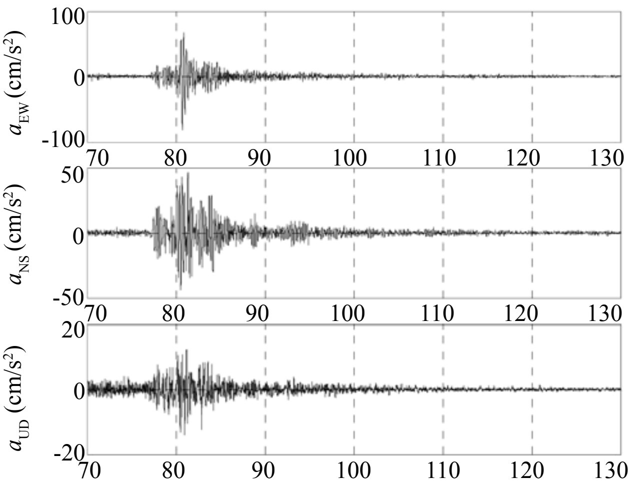

(b) At 3rd floor

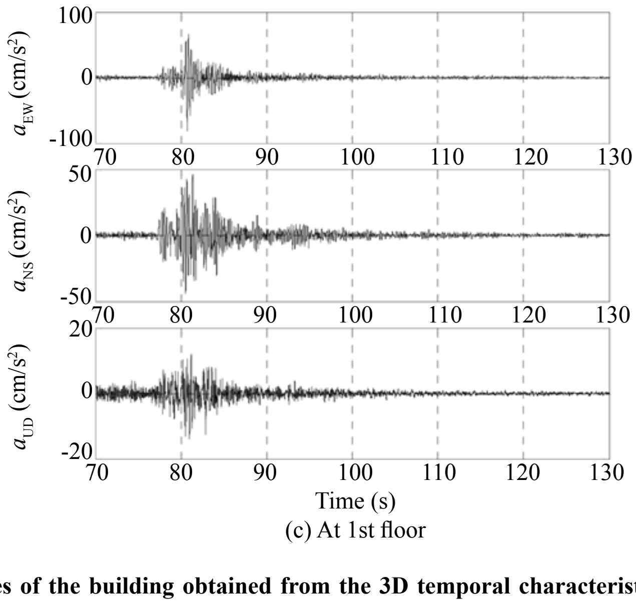

(c) At 1st floor

Fig. 8 Acceleration time histories of the building obtained from the 3D temporal characteristics analysis by using recordings during aftershock 1 of M_s6.4

Table 4 Monitored aftershock information

Earthquake name	Time	Magnitude	Epicenter	Epicentral distance
Aftershock 1	May 25,2008	M_s6.4	Qingchuan	90 km

Table 5 PGA information about aftershock 1

Floor No.	Translational components	Peak values (cm/s^2)	Occurrence time(s)
4	EW	183.626	80.727
	NS	119.497	80.68
	UD	-179.213	80.66
3	EW	-152.744	80.72
	NS	108.624	80.68
	UD	-41.423	80.663
1	EW	-81.985	80.723
	NS	46.812	81.333
	UD	-14.015	80.99

Table 6 Comparison of periods

Direction	Fundamental periods of the structure	Ground predominant period from nearby stations during aftershock M_s 6.4
EW	0.197	0.2957
NS	0.192	0.2957
Torsion	0.192	0.1601

3.2 Structural responses during May 25 aftershock of M_s6.4

Acceleration responses of the office building were recorded in series aftershocks of the earthquake by sensors. Each of the responses had three components and the sensors were installed in the middle room of each floor. The acceleration responses, captured during the largest May 25 aftershock of M_s 6.4, were analyzed by using 3D temporal characteristics analysis. The acceleration responses are shown in Fig. 8; and the basic information of aftershock 1 is provided in Tables 4 to 6. From Table 6, note that the fundamental period of the structure is considerably different from the predominant periods of the nearby ground motions, both during the major earthquake and its aftershocks. This could be why this office building was only slightly damaged in a series of strong ground shakings.

The jerk responses at the 1st and 2nd floors during aftershock 1 are shown in Fig. 9. PGAs and their recorded occurrence times as well as the accelerations integrated from the jerk responses are provided in Table 7, respectively. Figure 10 shows a comparison of the recorded acceleration response and the acceleration integrated from the jerk response during aftershock 1. Note that the maximum difference of PGAs between the recorded and integrated from jerk response was as high as about 49%, while the dissimilarity of their occurrence time was relatively small. In general, the time history curves shows good agreement with each other in intervals where peak values occurred, but the differences during other intervals was large, which may have been caused by noise. These differences may also have been caused by using an inappropriate filtering frequency band during data processing. Peak values and occurrence time of jerk recorded during aftershock 1 and the differentiated jerk from recorded acceleration are provided in Table 8. Figure 11 shows comparisons of recorded jerk response in aftershock 1 and the differentiated jerk. From Table 8 and Fig.11, it is seen that the biggest difference of peak jerks were reached at 30%, while the occurrence times show a good consistency. The time histories of the jerks coincide well with each other in intervals where peak values occurred. This observation is similar to the acceleration comparisons described above.

3.3 Three dimensional temporal characteristics analyses of the structural responses

3.3.1 Acceleration and velocity characteristics

Comparisons of a_T, a_N, $|\boldsymbol{a}|$, $|\boldsymbol{v}|$, and $|\boldsymbol{d}|$ of the recorded structural responses are shown in Fig.12 and Table 8. The kinematic relationship between them is discussed in the following sections. From Fig.12 and Table 8, when the RC frame structure was excited under aftershock 1, a_N and $|\boldsymbol{a}|$ had almost the same amplitude at the highest maxima; and the a_N and $|\boldsymbol{a}|$ arrived at their peak values at nearly the same instant. For example, the peaks of a_N and $|\boldsymbol{a}|$ on the 1st floor both arrived at 80.71s; while a_T had much less amplitude than $|\boldsymbol{a}|$ over the entire time interval. Another interesting observation is between a_T and a_N as shown in Fig.12 and Table 8; i.e., most positive a_N peak values precede positive a_T peaks. Furthermore, it was often observed that the peaks of a_N occurred at zero points of a_T. The relationship between a_T, a_N, $|\boldsymbol{a}|$ at different floors shows similar tendencies.

Figure 12 shows that $|\boldsymbol{v}|$ always increases in the phase of positive a_T and decreases in the phase of negative a_T. The above observation suggests that the high ground motion acceleration do not always correspond to large velocity or displacement. Instead, a large or long-lasting positive a_T component may be more vulnerable than the peak values of the EW, NS, and UD acceleration components. Another interesting observation from Table 9 is that both the velocity norm $|\boldsymbol{v}|$ and the displacement norm $|\boldsymbol{d}|$ at the same floor arrived at their peak values at the same instant.

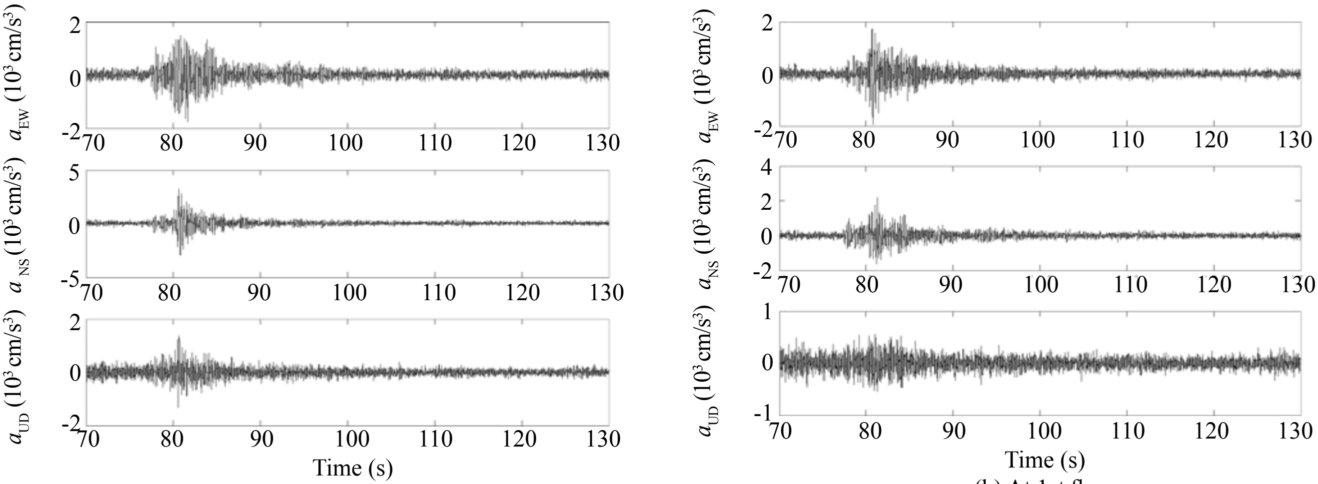

(a) At 2nd floor (b) At 1st floor

Fig. 9 Time histories of Jerks during aftershock 1 of M_s6.4

Table 7 Comparison of the recorded and integrated peak acceleration information

Floor No.	Translational components	Recorded		Integrated	
		Peak values (cm/s^2)	Occurrence time (s)	Peak values (cm/s^2)	Occurrence time(s)
2	EW	98.38	80.69	67.49	80.54
	NS	113.46	80.74	142.66	80.75
	UD	--	--		--
1	EW	81.99	80.72	78.61	80.74
	NS	46.81	81.33	69.74	81.24
	UD	14.02	80.99	18.67	82.88

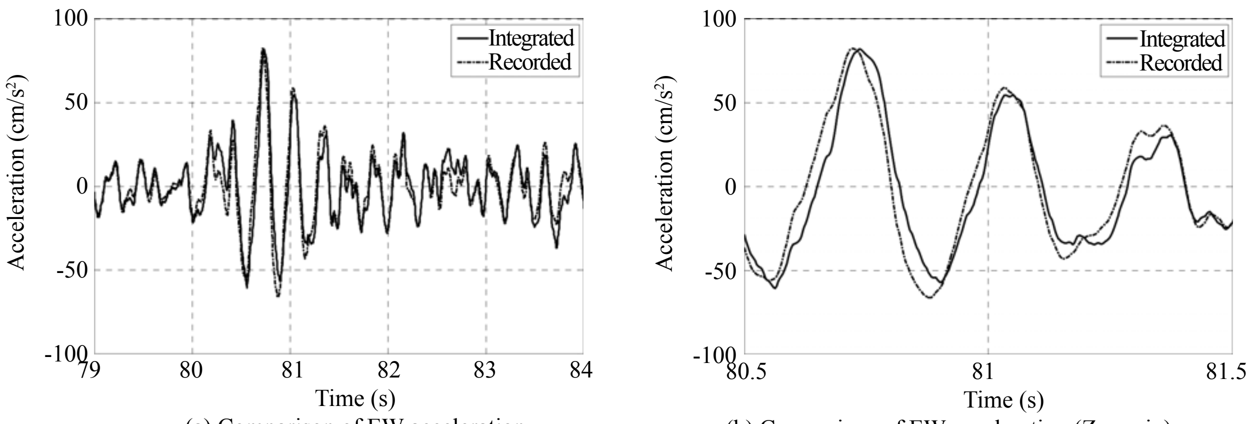

(a) Comparison of EW acceleration (b) Comparison of EW acceleration (Zoom in)

Fig. 10 Comparison of EW accelerations on the 1st floor

Table 8 Comparison of jerk responses

Floor No.	Translational components	Recorded		Differentiated	
		Peak values (cm/s^3)	Occurrence time(s)	Peak values (cm/s^3)	Occurrence time(s)
2	EW	1773.99	81.68	2242.40	81.68
	NS	3263.67	80.68	2750.75	80.68
	UD	--	--	--	--
1	EW	1964.29	80.79	2055.40	80.80
	NS	2218.38	81.31	1536.40	81.36
	UD	578.20	81.03	557.18	80.93

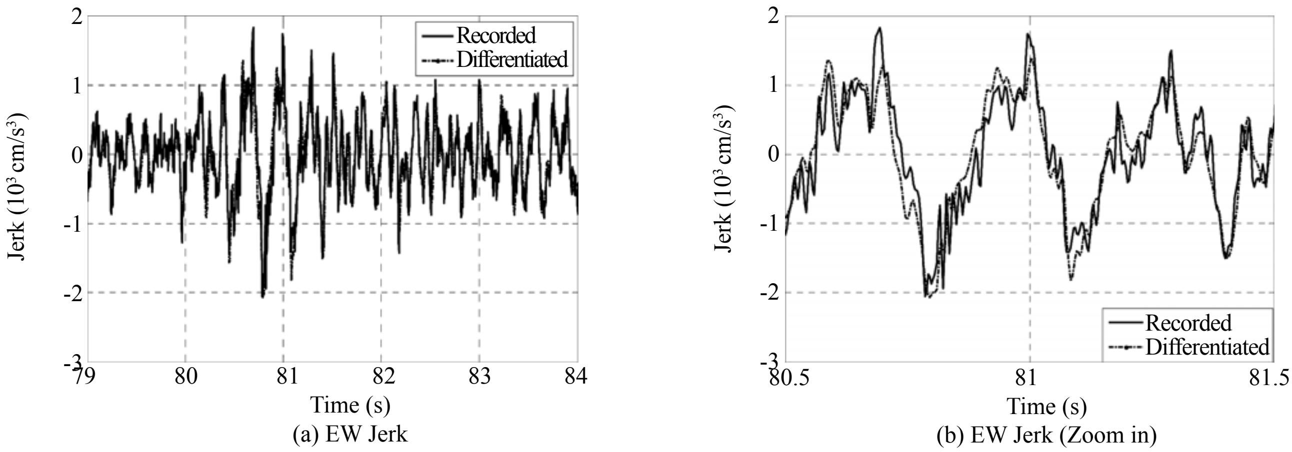

Fig. 11 Comparison of EW Jerk on the 1st floor

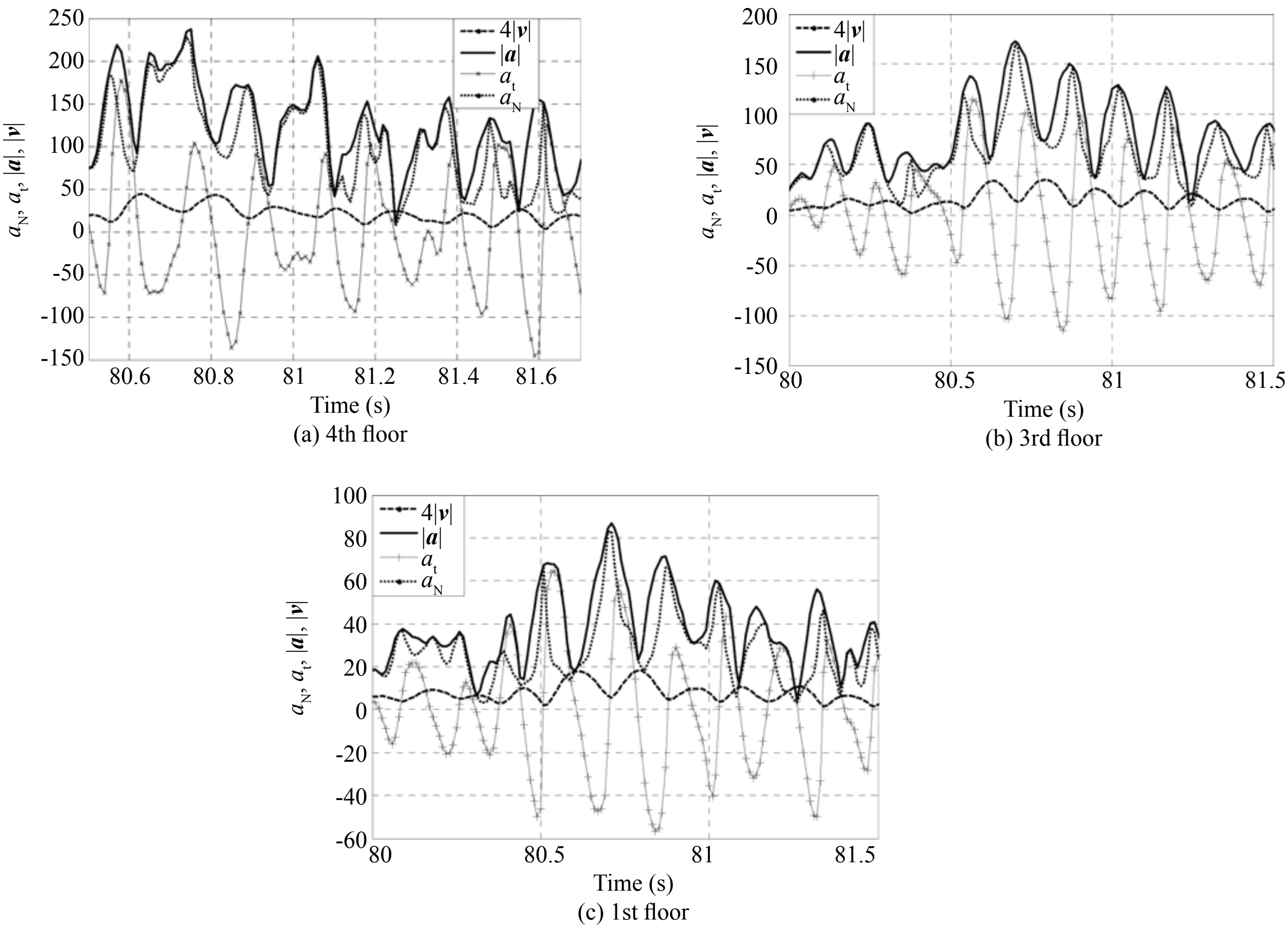

Fig. 12 Comparison of a_T, a_N, |*a*| and |*v*| at different floors during aftershock 1 (a_T (cm/s²), a_N (cm/s²), |*a*| (cm/s²) and |*v*| (cm/s))

3.3.2 Characteristics of the temporal curvature

Figure 13 shows that κ and a_N vary with the same tendencies and are very similar. Furthermore, their maxima always corresponds to the minimum of |***v***|, and their minima always corresponds to the maximum of |***v***|. This implies that every curvature pulse results in an increase of normal acceleration and a loss of some velocity. This is in good agreement with the discussion above.

Temporal curvature in units of time κ_t was obtained by multiplying |***v***| by κ. From Fig.13, note that pulses κ_t and κ vary in phase; but their amplitudes were very different. The large difference in their amplitudes shows that the influence of velocity was significant. It

Table 9 Comparison of responses during aftershock 1

Floor No.	Responses	Time (s)	Peak values
4	Positive a_T	80.580	176.898 cm/s^2
	Negative a_T	81.590	-145.831 cm/s^2
	a_N	80.740	228.260 cm/s^2
	$\|\boldsymbol{a}\|$	80.750	237.468 cm/s^2
	$\|\boldsymbol{v}\|$	80.630	14.833 cm/s
	$\|\boldsymbol{d}\|$	80.630	0.049 cm
3	Positive a_T	80.570	114.989 cm/s^2
	Negative a_T	80.850	-114.680 cm/s^2
	a_N	80.700	170.103 cm/s^2
	$\|\boldsymbol{a}\|$	80.700	172.694 cm/s^2
	$\|\boldsymbol{v}\|$	80.790	14.019 cm/s
	$\|\boldsymbol{d}\|$	80.790	0.047 cm
1	Positive a_T	80.540	64.652 cm/s^2
	Negative a_T	80.840	-56.439 cm/s^2
	a_N	80.710	83.234 cm/s^2
	$\|\boldsymbol{a}\|$	80.710	86.572 cm/s^2
	$\|\boldsymbol{v}\|$	80.610	8.963 cm/s
	$\|\boldsymbol{d}\|$	80.610	0.030 cm

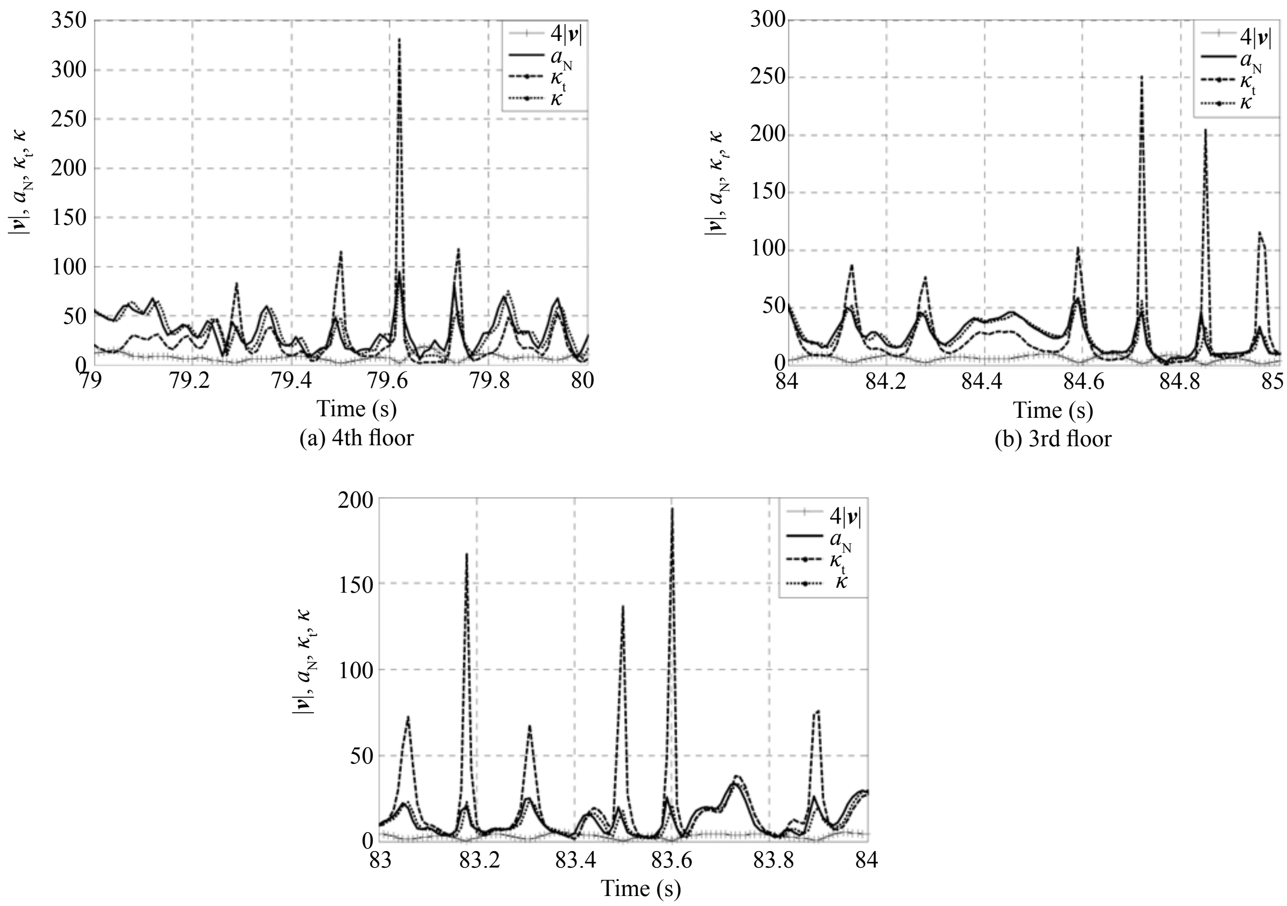

(a) 4th floor (b) 3rd floor (c) 1st floor

Fig. 13 Comparison of κ, κ_t, a_N and $|v|$ for different floors during aftershock 1 (κ (rad/cm), κ_t (rad/s), a_N (cm/s^2) and $|v|$ (cm/s))

is interesting to note that the time interval within which the highest a_N and κ occurred does not correspond to when the highest κ_t occurred; the highest a_N and κ often corresponded to a low or lower κ_t. Compared to both a_N and κ, $|\boldsymbol{v}|$ had a very small amplitude.

The relationship among κ, κ_t, a_N, and $|\boldsymbol{v}|$ at every floor shows the same trend when excited by aftershock 1.

3.3.3 Characteristics of temporal torsion

The temporal torsion time histories at different floors of the building under aftershock 1 are illustrated in Fig.14, from which some characteristics of the temporal torsion of aftershock 1 are summarized in Table 10.

Note that γ appears only in a limited time interval; and its effective γ duration and the highest temporal torsion pulse value both increase as the floor number of the building increases.

Figure 15 provides comparisons of κ, γ, γ_t, and $|\boldsymbol{v}|$ of the building under aftershock 1, where the kinetic relationship of κ, γ, γ_t, and $|\boldsymbol{v}|$ at all floors shows the same tendency. For example, the pulses of γ and γ_t always occurred simultaneously; further, they often occurred at a time of high velocity, which was the opposite of the κ pulses. γ and κ were in mutually opposite directions; that is to say, the curvature pulse corresponded to the torsion valleys and its valleys corresponded to the torsion pulse. This observation was also made by Tong and Lee (1999).

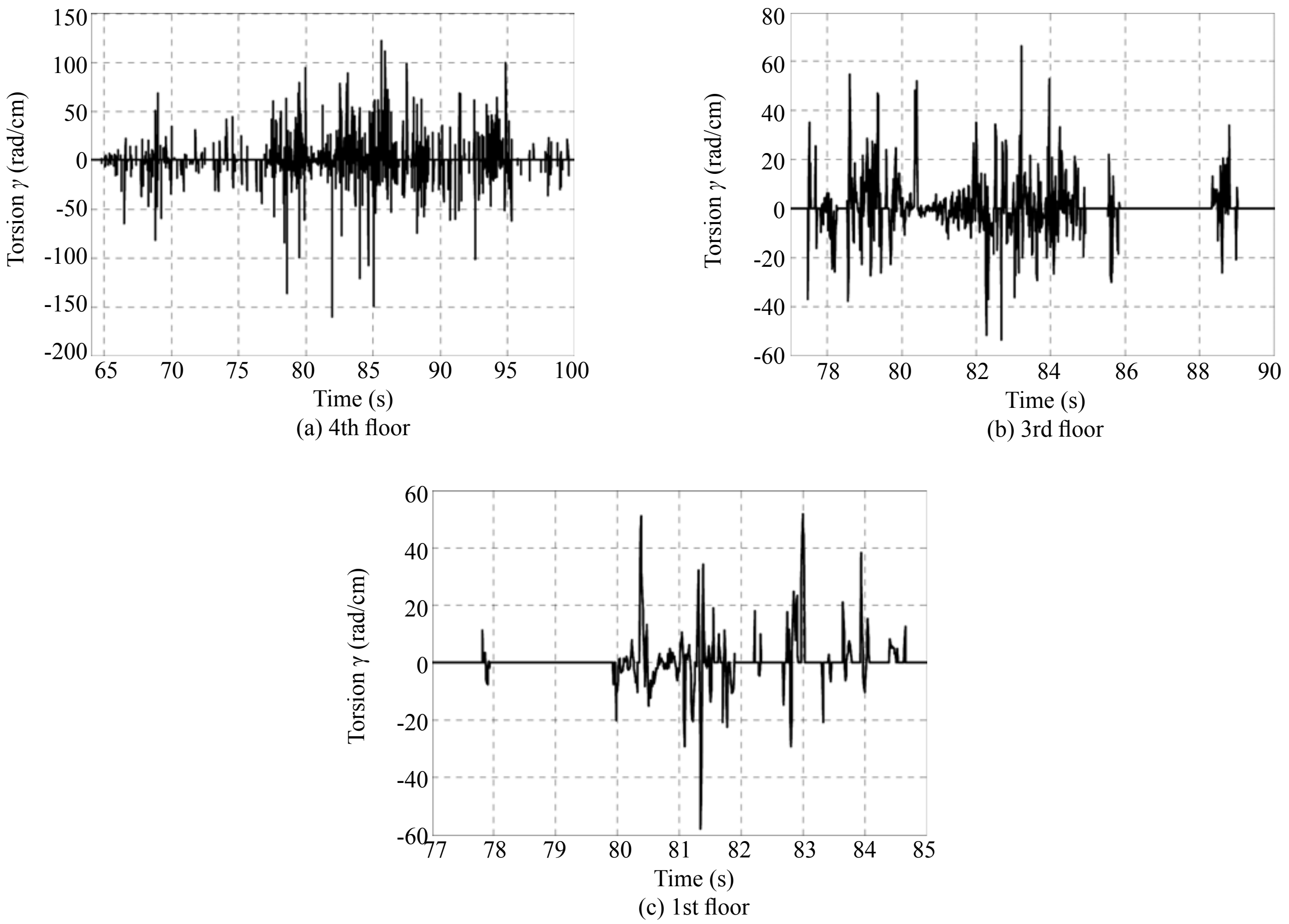

Fig. 14 Temporal torsion γ for different floors under aftershock 1

Table 10 Characteristics of the temporal torsion under aftershock 1

Floor No.	Time interval of non-zero γ (s)	Highest temporal torsion pulse	
		Value (rad/cm)	Occurrence time (s)
1st	77.8 – 85.0	57.71	81.35
3rd	77.4 – 89.1	66.16	83.22
4th	64.8 – 99.6	160.2	81.97

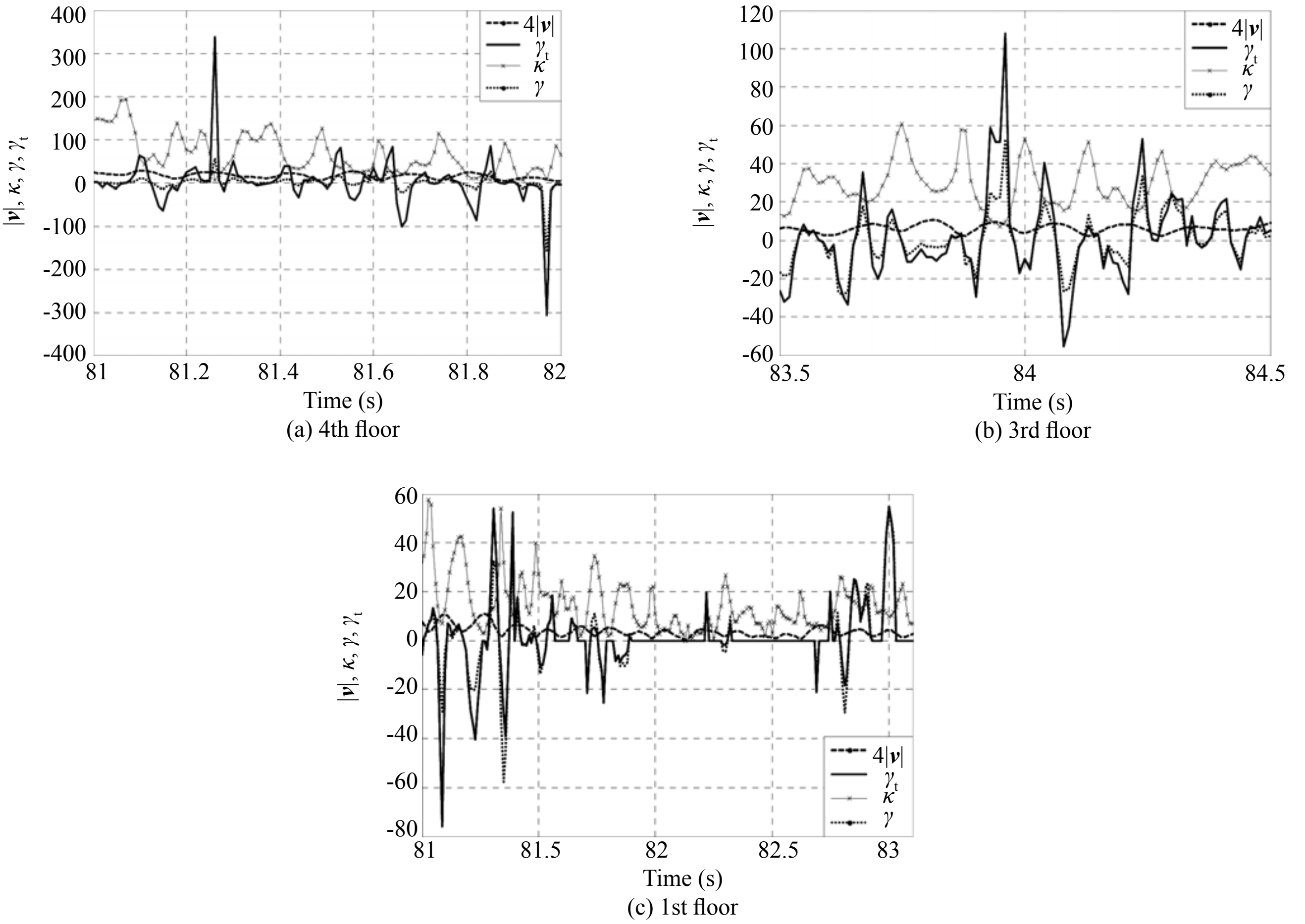

Fig. 15 Comparison of κ, γ, γ_t and $|v|$ for different floors under aftershock 1 (κ (rad/cm), γ (rad/cm), γ_t (rad/s)and $|v|$ (cm/s))

4 Discussions and findings

This paper summarizes the results of 3D temporal characteristics analyses that were carried out on ground motions from both the main shock and the largest M_s6.4 aftershock of Wenchuan earthquake on the acceleration responses of a RC frame structure. The 3D temporal characteristics were analyzed in terms of the instantaneous tangential acceleration a_T and normal acceleration a_N; Euclidean norm vectors of acceleration $|\boldsymbol{a}|$, velocity $|\boldsymbol{v}|$ and displacement $|\boldsymbol{d}|$; and temporal curvatures κ and κ_t, and temporal torsions γ and γ_t. From comparisons of the recorded responses and integrated from the recorded jerk responses, some significant findings are as follows:

(1) The relationship of a_T, a_N, $|\boldsymbol{a}|$, $|\boldsymbol{v}|$, and $|\boldsymbol{d}|$ for ground motions from the main shock of the Wenchuan earthquake was similar:

(a) the peak of $|\boldsymbol{d}|$ occurred later than the peak of $|\boldsymbol{a}|$, and was followed by the peak of $|\boldsymbol{v}|$;

(b) the $|\boldsymbol{a}|$ and the absolute value of a_T often arrived at their peaks almost simultaneously;

(c) the peak of a_N always occurred ahead of a_T; furthermore, peaks of a_N often corresponded to zero points of a_T;

(d) the $|\boldsymbol{v}|$ always increased with the positive a_T and $|\boldsymbol{v}|$ always decreased with the negative a_T. However, during aftershock 1, the relationship of a_T, a_N, $|\boldsymbol{a}|$, $|\boldsymbol{v}|$, and $|\boldsymbol{d}|$ for the structural response was different from the ground motions. This implies that their 3D characteristics rules were different from each other and depended on relevant conditions.

(2) The relationships of κ, κ_t, a_N, and $|\boldsymbol{v}|$ to the seismic responses of the structure and ground motions have the same tendency. κ and a_N approach each other. Furthermore, the maxima of κ and a_N always corresponded to the minimum of $|\boldsymbol{v}|$. This implies that every curvature pulse resulted in an increase of normal acceleration and a loss of some velocity. Pulses κ_t and κ varied with time in phase; but their amplitudes differed considerably from each other. It is interesting to note that higher a_N and κ often corresponded to lower κ_t.

(3) Temporal torsion of seismic responses of the structure and ground motions showed the same behaviors, i.e., the pulses of γ and γ_t always occurred at the same time and often within the region of higher velocity, which was opposite to the pulses γ. Another interesting observation of seismic responses of the structure was that γ was only distributed in a very short time interval for all floors; and the effective γ duration

and the highest temporal torsion pulse value both increased as the floor number of the building increases.

(4) The time instant when the peak values of acceleration time history records occurred and the peak acceleration response both agreed well with those integrated from the recorded jerk response. Also, the time intervals agreed well with the jerk that was differentiated from the recorded acceleration response, except for the values of the peak jerks of the time history of the recorded jerk response. There were some differences that may have been caused by the differentiation or integration between the calculated jerk and acceleration. This suggests that better data acquisition and processing are required in future monitoring of strong ground accelerations as well as jerks.

Further research will mainly focus on how to find the relationship between the 3D temporal characteristics and the damage patterns of building structures under strong ground motions. Both numerical simulation, past earthquake damage observations and laboratory tests will be conducted in the future.

Notations

The following symbols are used in this paper:

a_T = instantaneous tangential acceleration;

a_N = instantaneous normal acceleration;

$|\boldsymbol{a}|$ = Euclidean norm of acceleration vector;

$|\boldsymbol{v}|$ = Euclidean norm of velocity vector;

$|\boldsymbol{d}|$ = Euclidean norm of displacement vector;

κ = Temporal curvature;

κ_t = Temporal curvature in units of time;

γ = Temporal torsion;

γ_t = Temporal torsion in units of time;

S =3D displacement experienced by the point.

Acknowledgements

The authors gratefully acknowledge the China National Ground Motion Monitoring Center for providing the ground motion records, and the joint financial support of the National Natural Science Foundation of China (Project No. 50678161), the National Major Basic Research 973 Program (No. 2007CB714205), the Science and Technology Support Program (No. 2006BAC13B02-0301) of the Ministry of Science and Technology of P.R. China, and the Basic Science Research Foundation (Institute Director foundation) Program through the Institute of Engineering Mechanics, CEA.

References

Dai Junwu, Qi Xiaozhai, Tong Mai and Lee GC (2004), "3D Temporal Characteristics Analysis for CHI-CHI Earthquake Ground Motion," *13th World Conference on Earthquake Engineering*. Paper No. 2858.

Dai Junwu, Qi Xiaozhai, Wang Yanru, Lee GC and Tong Mai (2008) "3D Temporal Characteristics Analyses for Seismic Responses of Structures," *14th World Conference on Earthquake Engineering*. Paper No. S06-010.

Lee GC, Tong M and Tao R (2000), "Temporal Characteristics of Chi-Chi Earthquake Ground Motion and Their Possible Implications on Structural Damages," *International Workshop on Annual Commemoration of Chi-Chi Earthquake*.

Tong Mai and Lee GC (1999), "3D Temporal Characteristics of Earthquake Ground Motion at a Single Point," *Journal of Engineering Mechanics*, ASCE, **125**(10): 1099–1105.

Tong Mai, Qi Jinchen, and Lee GC (2002), "Temporal a_N and a_T in Earthquake Ground Motion Analysis," *Journal of Engineering Mechanics*, ASCE, **128**(5): 502–510.

Tong Mai, Rzhevsky Vladimir, Lee GC, Qi Jincheng, Dai Junwu and Qi Xiaozhai (2006), "Near-fault Ground Motions with Prominent Acceleration Pulses Part 1: Evaluation of Pulse Characteristics and the Structural Damage Potential," *4th International Conference on Earthquake Engineering (4ICEE),* Paper No. 104.